Diarch Symmetry of the Vascular Bundle in Arabidopsis Root Encompasses the Pericycle and Is Reflected in Distich Lateral Root Initiation[1][W]

Boris Parizot, Laurent Laplaze, Lilian Ricaud, Elodie Boucheron-Dubuisson, Vincent Bayle, Martin Bonke, Ive De Smet, Scott R. Poethig, Yka Helariutta, Jim Haseloff, Dominique Chriqui, Tom Beeckman, and Laurent Nussaume*

Laboratoire de Biologie du Développement des Plantes, Department of Plant Biology and Environmental Microbiology, The Institute of Environmental Biology and Biotechnology, Direction des Sciences du Vivant, Commissariat à l'Energie Atomique, Centre National de la Recherche Scientifique, Université Aix-Marseille, Saint Paul lez Durance F–13108, France (B.P., L.R., V.B., L.N.); Department of Plant Systems Biology, Root Development Group, Flanders Interuniversity Institute of Biotechnology and Department of Molecular Genetics, Ghent University, B–9052 Ghent, Belgium (B.P., I.D.S., T.B.); Equipe Rhizogenèse, Université Mixte de Recherche DIA-PC, Institut de Recherche pour le Développement, 34394 Montpellier cedex 5, France (L.L.); Department of Plant Sciences, University of Cambridge, Cambridge CB2 3EA, United Kingdom (L.R., J.H.); Université Pierre et Marie Curie, F–75252 Paris cedex 05, France (E.B.-D., D.C.); Plant Molecular Biology Laboratory, Institute of Biotechnology, University of Helsinki, FI–00014 Helsinki, Finland (M.B., Y.H.); and Carolyn Lynch Laboratory, Department of Biology, University of Pennsylvania, Philadelphia, Pennsylvania 19104 (S.R.P.)

The outer tissues of dicotyledonous plant roots (i.e. epidermis, cortex, and endodermis) are clearly organized in distinct concentric layers in contrast to the diarch to polyarch vascular tissues of the central stele. Up to now, the outermost layer of the stele, the pericycle, has always been regarded, in accordance with the outer tissue layers, as one uniform concentric layer. However, considering its lateral root-forming competence, the pericycle is composed of two different cell types, with one subset of cells being associated with the xylem, showing strong competence to initiate cell division, whereas another group of cells, associated with the phloem, appears to remain quiescent. Here, we established, using detailed microscopy and specific *Arabidopsis thaliana* reporter lines, the existence of two distinct pericycle cell types. Analysis of two enhancer trap reporter lines further suggests that the specification between these two subsets takes place early during development, in relation with the determination of the vascular tissues. A genetic screen resulted in the isolation of mutants perturbed in pericycle differentiation. Detailed phenotypical analyses of two of these mutants, combined with observations made in known vascular mutants, revealed an intimate correlation between vascular organization, pericycle fate, and lateral root initiation potency, and illustrated the independence of pericycle differentiation and lateral root initiation from protoxylem differentiation. Taken together, our data show that the pericycle is a heterogeneous cell layer with two groups of cells set up in the root meristem by the same genetic pathway controlling the diarch organization of the vasculature.

The Arabidopsis (*Arabidopsis thaliana*) root displays two different levels of tissue organization: a concentric organization formed by the ground layers (endodermis/cortex) and the epidermis, and a bilateral symmetry of the diarch vascular bundle consisting of two poles of xylem elements and two poles of phloem elements (Dolan et al., 1993). The outermost layer of the central cylinder or stele is the pericycle, which is traditionally regarded as one extra concentric layer. Indeed, all pericycle cells share common physical properties and form a unique layer of regularly shaped cells in contact with each other by their tangential cell walls (Dolan et al., 1993). During embryogenesis, the pericycle initiates from the same subset of initial cells as the rest of the stele and can be recognized as a distinct concentric layer already formed at the heart stage, even before the endodermal and cortical cell files become specified (Scheres et al., 1994). However, many studies in different species have emphasized the differences between pericycle cells according to their position adjacent to the xylem or the phloem poles in terms of cell division competence (Dubrovsky et al.,

[1] This work was supported by the Commissariat à l'Energie Atomique, the Marie Curie Foundation, the Institut de Recherche pour le Développement, and Tournesol (bilateral grant no. 11532RD to L.L. and T.B.).

* Corresponding author; e-mail lnussaume@cea.fr.

The author responsible for distribution of materials integral to the findings presented in this article in accordance with the policy described in the Instructions for Authors (www.plantphysiol.org) is: Laurent Nussaume (lnussaume@cea.fr).

[W] The online version of this article contains Web-only data.
www.plantphysiol.org/cgi/doi/10.1104/pp.107.107870

2000), cell cycle progression (Beeckman et al., 2001), cell size (Casero et al., 1989; Dubrovsky et al., 2000), cell surface arabinogalactan-protein distribution and cell wall thickening (Dolan and Roberts, 1995; Casero et al., 1998; Majewska-Sawka and Nothnagel, 2000), methyl blue staining (Toriyama, 2005), plasmodesmatal connections (Wright and Oparka, 1997; Complainville et al., 2003), physical disposition against endodermis cells (Dolan et al., 1993), microtubule content (Hardham and Gunning, 1979), and marker gene expression (Laplaze et al., 2005; Mahonen et al., 2006).

Lateral root development in dicotyledonous plants occurs postembryonically from pericycle cells and guarantees the spatial development and plasticity of root systems (Torrey, 1950; Celenza et al., 1995; Malamy, 2005). Auxin is unambiguously the main signal inducing pericycle cells to enter lateral root initiation (Casimiro et al., 2003; De Smet et al., 2007). Interestingly, only the subset of the pericycle cells associated with xylem poles is involved in lateral root initiation, thus reinforcing the idea that the pericycle is a heterogeneous cell layer. The mechanisms controlling pericycle cell determination and competence for lateral root initiation are currently unknown. Here, we demonstrate, using cytological approaches, that there are two distinct types of pericycle cells. We describe a new enhancer trap line marker that visualizes this distinction already as early as in the root meristem. Finally, we used genetic approaches to identify mutants altering quantitatively and/or qualitatively pericycle organization. Our data substantiate the existence of two types of pericycle cells set up in the root meristem. Furthermore, our data show that diarch determination of both the pericycle and the vasculature are regulated by a common genetic pathway.

RESULTS

Pericycle Is Made of Two Different Cell Types as Revealed by Cytological Analyses

Only few reports have examined the ultrastructural features of the Arabidopsis root pericycle (Dolan et al., 1993; Wright and Oparka, 1997) and a detailed comparison between pericycle cells at the xylem poles versus those at the phloem poles is currently lacking. Therefore, the cytological aspects of both groups of pericycle cells were analyzed by transmission electron microscopy (TEM) in plants grown under normal conditions, as well as under lateral root-inhibiting and lateral root-inducing conditions. Seedlings were germinated on Murashige and Skoog and 1-*N*-naphthylphthalamic acid (NPA) medium. At 72 h after germination (DAG), part of the seedlings on NPA was transferred to α-naphthalene acetic acid (NAA) and incubated for 10 h. In this way, three different samples were obtained: untreated roots, roots prevented from lateral root initiation (NPA), and roots of which the entire pericycle is synchronously induced for lateral root initiation by NAA treatment (Himanen et al., 2002). In all samples, sections for comparative TEM analysis were made through the distal part of the differentiation zone.

In untreated roots, the protoxylem-pole pericycle cells displayed meristematic features with frequently three or more vacuoles and a dense cytoplasm containing numerous electron-dense ribosomes (Fig. 1A). At the phloem pole, all pericycle cells presented a single and large central vacuole and a parietal cytoplasm with less ribosomes, characteristic of more differentiated status (Fig. 1B). An opposite situation was found for NPA-treated seedlings. Whereas the protoxylem-pole pericycle cells reduced their meristematic appearance by acquiring one large central vacuole and a reduction in the number of ribosomes (Fig. 1C), the protophloem-pole pericycle cells showed, under these conditions, meristematic appearance with a densely stained cytoplasm, loss of the central vacuole in most of the cells, and enrichment in endoplasmic reticulum (Fig. 1D). In some sections, we could even notice the result of a recent periclinal cell division event by the appearance of a thin cell wall subdividing former pericycle cells into two daughter cells (Fig. 1D, arrowheads). These divisions are, however, rare and never give rise to lateral root formation. After transfer to NAA, the situation was pushed over again with the two types of pericycle cells reacting in an opposite manner. At the xylem poles, pericycle cells clearly became meristematic with the development of numerous small vacuoles, nuclei with large nucleoli (Fig. 1E), whereas phloem pericycle cells reacquired parietal cytoplasm and a central vacuole (Fig. 1F). These analyses indicate that both types of pericycle cells react differentially and even in an opposite way to lateral root-inhibiting versus lateral root-inducing conditions.

Pericycle Bilateral Heterogeneity Already Occurs in Stele Initials

Having demonstrated the clear difference between protoxylem-pole and phloem-pole pericycle cells, we used GAL4 enhancer trap lines (see ''Materials and Methods'') as markers to study further the organization of the root pericycle. The J0121 line (Laplaze et al., 2005) marks pericycle cells associated with xylem poles (Fig. 2, A–H), starting from the elongation zone above the root tip (Fig. 2C) and expanding in a basipetal direction throughout the root (Fig. 2B). J0121 GFP expression precedes protoxylem differentiation (data not shown) and is later closely associated with this tissue (Fig. 2E). Three contiguous pericycle cell files are expressing GFP (Fig. 2D), which are competent to divide and later form lateral root primordia (Kurup et al., 2005). J0121 GFP expression is down-regulated in nascent and developing lateral root primordia (Fig. 2F).

Another population of Arabidopsis GAL4 enhancer trap lines (Columbia [Col-0] background) was screened to identify novel pericycle markers. This led to the identification of the reporter line Rm1007, which expresses GFP specifically in the pericycle associated

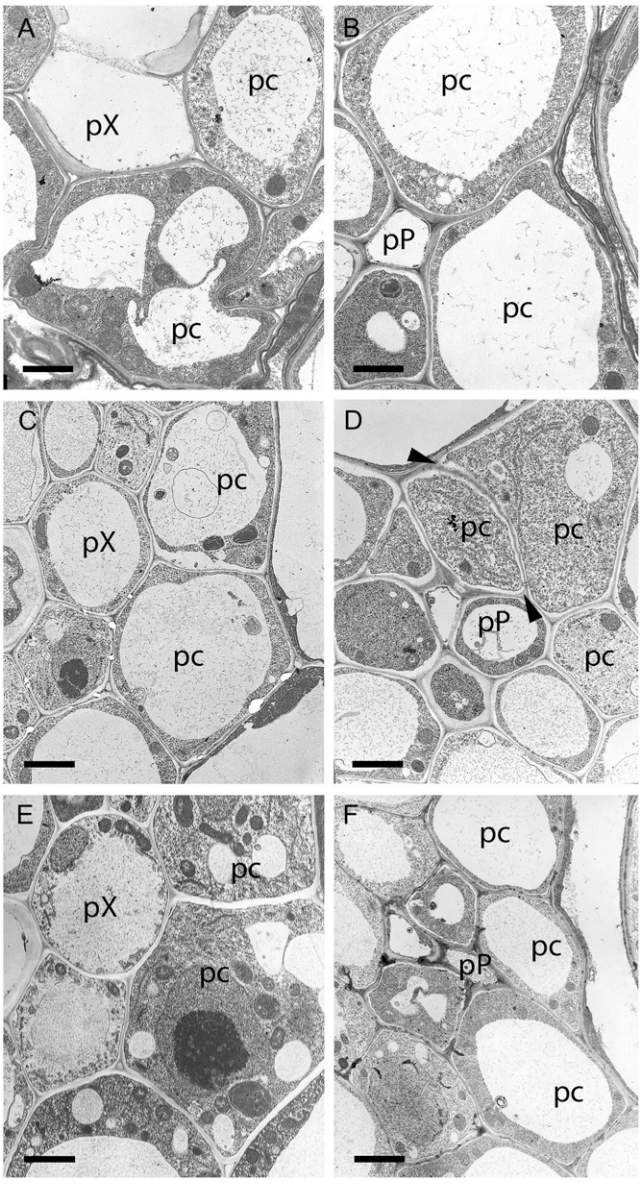

Figure 1. TEM analysis of pericycle cells. TEM analysis of pericycle cells at the protoxylem pole (A, C, and E) as compared to pericycle cells at the protophloem pole (B, D, and F) after growth on control medium (A and B), NPA (C and D), and NPA followed by 10 h of incubation on NAA (E and F). A newly formed periclinally oriented cell wall in a pericycle cell at the phloem pole on NPA is indicated by two black arrowheads. pc, Pericycle; pP, protophloem pole; pX, protoxylem pole. Bars = 3.5 μm (A–D); 3 μm (E and F).

with xylem poles (Fig. 2, I–N) and mainly in three contiguous pericycle files (Fig. 2L). Compared to J0121, GFP expression was detected earlier in the root tip, starting from the initials immediately above the quiescent center cells (Fig. 2, K and L). Furthermore, this expression pattern could be detected in heart-stage embryos (Fig. 2M). This early expression is comparable to the expression pattern observed in young lateral root primordia before emergence (Fig. 2J, arrow). It persists in older parts of the root where GFP remains exclusively expressed in the pericycle associated with xylem poles (Fig. 2N). Unlike J0121, expression is more intense in young tissues and fades away progressively in older parts (Fig. 2I). In conclusion, expression of the GFP enhancer trap marker in both J0121 and Rm1007 lines labeled a subset of cells in the pericycle, associated with the xylem poles, with Rm1007 labeling the xylem-pole pericycle from the first initials.

Lateral root initiation, which takes place in the pericycle cells facing xylem poles, is regulated by exogenous and endogenous signals (Malamy, 2005). Different experiments were performed to test whether pericycle cell specification was modified by stress, nutrient, and hormone conditions. Neither tested nutrient concentrations (phosphate, nitrate, and Suc) nor stress (wounding, heat shock, and drought) resulted in any obvious change of the GFP expression pattern in the J0121 line (see ''Materials and Methods''; data not shown). J0121 behavior was also tested against two major hormones involved in root development. Neither auxin, NPA (Fig. 2, G and H), nor cytokinin (Supplemental Fig. S1, A–D) treatments affected the GFP expression pattern of J0121. Similar results were observed with the Rm1007 line for NPA and NAA treatments (Fig. 2J; Supplemental Fig. S1, E and F). Therefore, even if these treatments induce (auxin; Celenza et al., 1995) or reduce (NPA and cytokinin; Reed et al., 1998; Lohar et al., 2004) root ability to initiate primordia, they appear to have no effect on the spatial organization of pericycle cells competent for lateral root initiation. We conclude that Rm1007 and J0121 patterns robustly delimit the subset of pericycle cells competent for lateral root initiation and are not perturbed by auxin or cytokinin treatment. This suggests that the specification of different pericycle cell types is not controlled by any of these signals.

Genetic Analysis Identifies New Mutants Altered in Pericycle Bilateral Organization

To get insight into the mechanisms that specify the different populations of pericycle cells, we performed a genetic screen on the J0121 enhancer trap line. For further analysis, J0121 was preferred instead of Rm1007 because variation in the intensity of the GFP was noticed in Rm1007 probably due to epigenetic regulations. Fifteen hundred independent F_2 progeny of ethyl methanesulfonate-mutagenized seedlings were screened to isolate mutants exhibiting qualitative or quantitative alteration of the GFP expression pattern. This led to the identification of 12 mutants showing different phenotypes related to J0121 expression: discontinuity, ectopic expression in the pericycle, ectopic expression outside the pericycle, and down-regulation of GFP expression. Interestingly, most of these mutants showed an alteration in their lateral root initiation ability (Supplemental Fig. S2). We have focused on two mutants showing a strong and stable phenotype with altered radial pattern of GFP expression in the pericycle, *lonesome highway* (*lhw*;

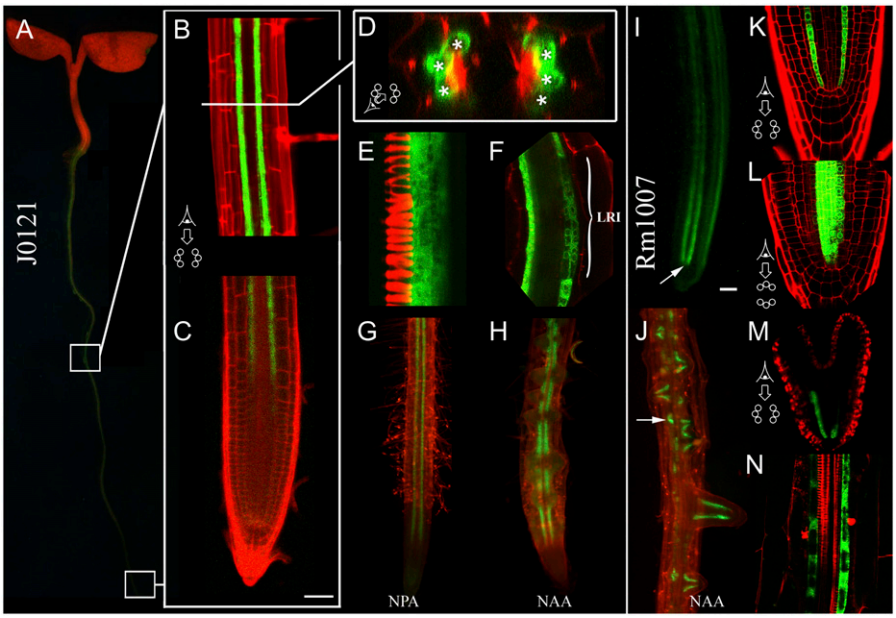

Figure 2. Histological analysis of heterogeneous GFP expression in Rm1007 and J0121 enhancer trap lines. A to H, J0121 analysis. A, Binocular imaging of a J0121 plantlet 5 DAG. B and C, Confocal imaging of mature part and apex, respectively; D, transversal section of mature part; E, enlargement of the protoxylem and the associated pericycle; F, lateral root initiation. G and H, Expression of the GFP in the root tip of a 5-DAG J0121 plantlet germinated on medium supplemented with 10^{-5} M NPA (G), on nonsupplemented medium for 2 d, and then transferred to medium supplemented with 10^{-5} M NAA for 24 h (H). Asterisks mark pericycle cells associated with xylem poles. I to N, Rm1007 analysis. I and J, Binocular imaging of a Rm1007 plantlet root tip 5 DAG, the arrow indicating the quiescent center (I); mature zone where lateral root formation is induced by transferring a plantlet germinated on nonsupplemented medium for 2 d to medium supplemented with 10^{-5} M NAA for 24 h (J). K to N, Confocal longitudinal imaging of Rm1007 in a protoxylem plan (K), in a plan parallel to the phloem in which can be seen three cell files of pericycle expressing GFP (L), during embryo heart-stage formation (M), and in the mature root (N). The eye symbol gives observation axis indication referring to the pericycle cells expressing GFP. Bars = 50 μm (C and I).

Fig. 3, D–F) and *impaired vasculature development* (*ivad*; Fig. 3, G–I), as compared with the J0121 marker line control (Fig. 3, A–C).

Pericycle Determination and Lateral Root Initiation Potency Are Intimately Correlated with Vascular Organization in the *lhw* Mutant

Two recessive mutant alleles of the previously reported *lhw* mutant (Ohashi-Ito and Bergmann, 2007) were identified in our screen and were therefore named *lhw6* and *lhw7*. Because the two alleles displayed a highly similar phenotype, we will refer to them as *lhw* mutations in this article. The *lhw* mutants present a reduction in primary root growth and in lateral root initiation density (37% and 47%, respectively; Supplemental Fig. S2). In contrast to the J0121 line, the *lhw* mutants showed only one strand of pericycle cells expressing GFP (Fig. 3F). Furthermore, sections made through the mature part of the root revealed that these lines develop only one-half of the vascular bundle (one xylem pole and one phloem pole) and fewer pericycle cells compared to the control (Fig. 3E; Supplemental Fig. S3). This reduction of the circumferential number of pericycle cells does not prevent lateral root formation (Supplemental Fig. S2). Loss of diarch organization starts from the meristematic region and is maintained throughout the whole root in these mutants. The number of cells belonging to the outer layers is not significantly different from those found in wild-type plants (Supplemental Fig. S3) and described previously (Dolan et al., 1993). No structural differences could be observed in the lateral root cap and the columella (data not shown) or at the level of the four quiescent center cells themselves as compared to the wild type (Fig. 3D). Confocal microscopy analysis revealed expression to be restricted to one strand of three contiguous pericycle cell files associated with the xylem pole along the whole root of the plant (Supplemental Fig. S4, A–C). As in J0121, GFP expression is detected before the protoxylem fully differentiates (data not shown). To summarize, *lhw* mutants only develop one-half of the vascular structures and the loss in diarch organization occurs before differentiation of the vascular elements. This in turn leads to a single strand of GFP-expressing pericycle cells in the J0121 marker line background.

To study the lateral root-forming capacity of the pericycle in *lhw* mutants, plants were germinated on medium supplemented with NPA and then transferred to medium supplemented with NAA to synchronously stimulate lateral root formation along the whole root of the plant, according to the lateral root-inducible system (Himanen et al., 2002; Vanneste et al.,

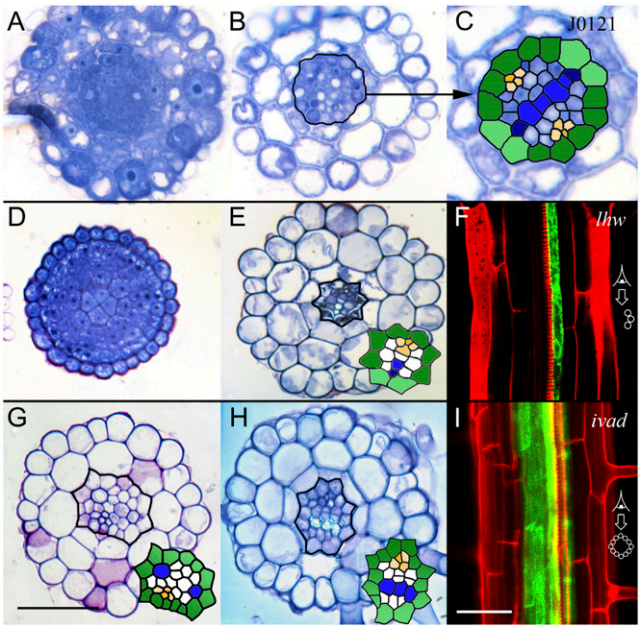

Figure 3. Histological study of stele alterations in *lhw* and *ivad* mutants. A to H, Transversal sections of 5-DAG embedded plants: C24 plants, respectively, in the differentiation zone and in mature parts of the root (A–C); *lhw* plants, respectively, at the level of the four quiescent center cells and in mature part of the root (D and E); and *ivad* plant in the mature part of the root (G and H). F and I, Longitudinal confocal imaging of *lhw* (F; one section) and *ivad* mutants (I; z-series stack superposition). Black lines on sections delimit scheme enlargement. Green, pericycle; blue and darker blue, xylem and protoxylem; orange, phloem poles. The eye symbol gives observation axis indication referring to the pericycle cells expressing GFP. Bars = 50 μm.

2005). Both the J0121 marker line and the mutants were initially checked for proper expression of GFP on NPA-supplemented medium and no obvious changes could be noticed (Fig. 4, A and C). Four DAG, plants were transferred to NAA, inducing divisions in the pericycle. Roots of wild-type plants show the common pattern described in the literature, with lateral roots emerging on both sides of the root along the two strands of GFP (i.e. pericycle cells associated with xylem poles; Fig. 4, B and D). In *lhw*, laterals only emerge from one side of the root following the unique strand of GFP. All the observed lateral roots emerged exclusively from the pericycle associated with xylem poles. This experiment demonstrates that pericycle cells competent for lateral root initiation remain exclusively adjacent to the xylem pole and express exclusively the J0121 GFP marker. Quantitative losses in vascular bundle and pericycle heterogeneity appear intimately correlated: There is a concomitant loss of diarch and bilateral structures in *lhw* mutants.

Protoxylem Differentiation Is Not Required for Pericycle Differentiation and Lateral Root Initiation

The recessive *ivad* mutant shows ectopic GFP expression in the root: GFP expression extends in the pericycle additionally to the normal pattern, above the differentiation zone in plants grown 4 to 5 DAG (Fig. 3I). Primary root growth is drastically reduced (Supplemental Fig. S2) and root gravitropism is altered (data not shown). Further analysis revealed that this mutant was dramatically impaired in vascular and endodermis development (Fig. 3, G and H). Fewer cells constitute the vascular bundle. Phloem and protoxylem development are altered, these tissues being partially or even fully absent (Fig. 3, G and H). In parts of the root where normal J0121 GFP expression was observed, the vascular bundle appears not to be affected by the mutation (data not shown). The endodermis also shows similar alterations (Fig. 3, G [absent] and H [partially absent]). However, regions with altered GFP patterning in the mutants were found where the endodermis was correctly formed. These aspects of the *ivad* phenotype highlight the intimate link between the correct diarch development of the vascular bundle and the proper bilateral symmetry of the pericycle.

Whereas the root phenotype of the *lhw* mutants clearly illustrated the relationship between xylem poles and lateral root initiation, we wondered whether impaired protoxylem differentiation of the *ivad* mutant would result in aberrant lateral root initiation. Differential interference contrast (DIC) microscopy analysis allows easy distinction between meta- and protoxylem elements in Arabidopsis roots, the first having reticulate and the latter helical cell wall thickening. DIC analysis of this mutant revealed that lateral root initiation could still proceed in regions where no protoxylem differentiated (Fig. 5, D–F). To confirm this observation, J0121 marker GFP expression and lateral root initiation were investigated in one mutant and one transgenic line, respectively, *ahp6* and *Pro$_{35S}$-VND7:SDRX*,

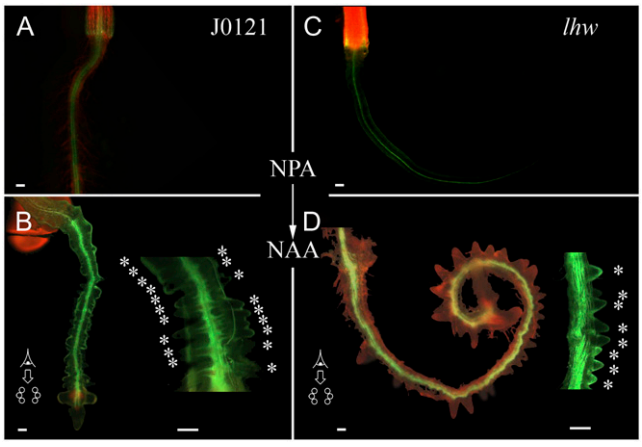

Figure 4. Lateral root initiation in *lhw* mutant. J0121 (A and B) and *lhw* (C and D) plants 3 DAG on medium supplemented with 10^{-5} M NPA (A and C) and then transferred 4 d on medium supplemented with 10^{-5} M NAA (B and D). Asterisks indicate lateral root emergence. The eye symbol gives observation axis indication referring to the pericycle cells expressing GFP. Bars = 100 μm.

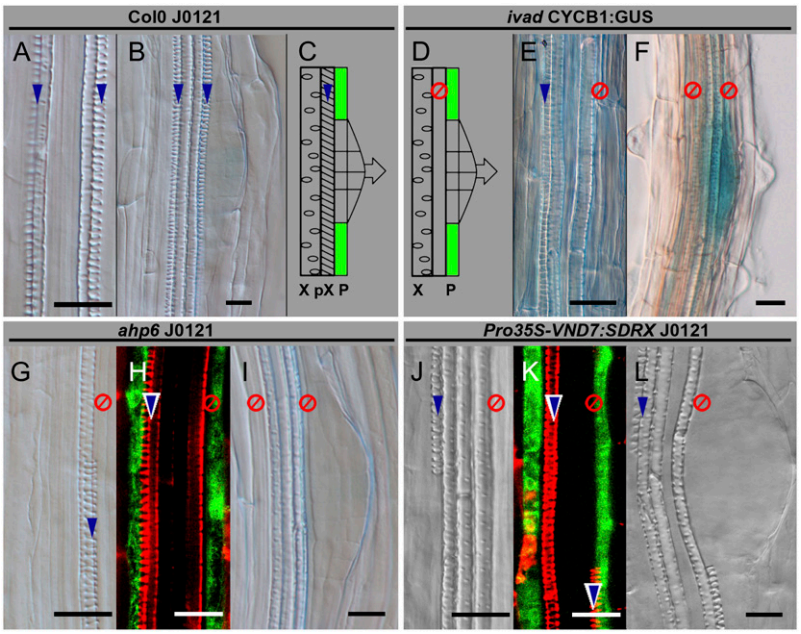

Figure 5. Lateral root initiation in *ivad*, *ahp6*, and *Pro*$_{35S}$*-VND7:SDRX* mutants does not require differentiated protoxylem. Lateral root initiation in relation to the presence or absence of fully developed protoxylem elements has been studied in Col-0 J0121 (A and B) and in three lines showing alteration in protoxylem differentiation: *ivad* (E and F), *ahp6* J0121 (G–I), and *Pro*$_{35S}$*-VND7:SDRX* J0121 (J–L). In Col-0 J0121, metaxylem is surrounded by protoxylem (A and C) and lateral root initiation happens in the pericycle adjacent to the protoxylem. In the three displayed mutants, absence of protoxylem surrounding metaxylem can be noticed (E, G, and J) and this absence prevents GFP expression neither in pericycles associated with xylem poles (H and K) nor in lateral root initiation (D, F, I, and L). Fully differentiated protoxylem presence is indicated with blue arrows; absence is indicated with the red symbol. P, Pericycle; pX, protoxylem; X, metaxylem. Bars = 20 μm.

in which affected protoxylem differentiation was already described (Kubo et al., 2005; Mahonen et al., 2006). The major defect in these mutants is the discontinuous differentiation of the protoxylem along the primary root. In *ahp6* and *Pro*$_{35S}$*-VND7:SDRX*, J0121 GFP maker expression and lateral root initiation can happen in front of xylem poles without any need for a differentiated protoxylem (Fig. 5, G–I and J–L). Moreover, lateral roots emerge with the same frequency in regions with or without a differentiated protoxylem in *aph6* (data not shown). These results show that a differentiated protoxylem element within the xylem pole (Fig. 5, A–C) is not required for proper pericycle differentiation regarding J0121 GFP expression and lateral root initiation.

Suppression of Vascular Heterogeneity in the *wol* Mutant Correlates with Loss of Heterogeneity in the Pericycle

To determine whether the qualitative loss in vasculature heterogeneity has consequences on the ability of pericycle cells to divide and form new lateral roots, we used the *wol* mutant (Scheres et al., 1995). Indeed, this mutant presents a defect in procambial cell specification, giving rise to a reduced number of cells. As a consequence, the phloem is not determined and only protoxylem tissues differentiate in the vascular bundle (Fig. 6E; Scheres et al., 1995; Mahonen et al., 2000).

GFP expression in *wol* J0121 cross spreads over the whole pericycle compared to the control (Fig. 6, A and

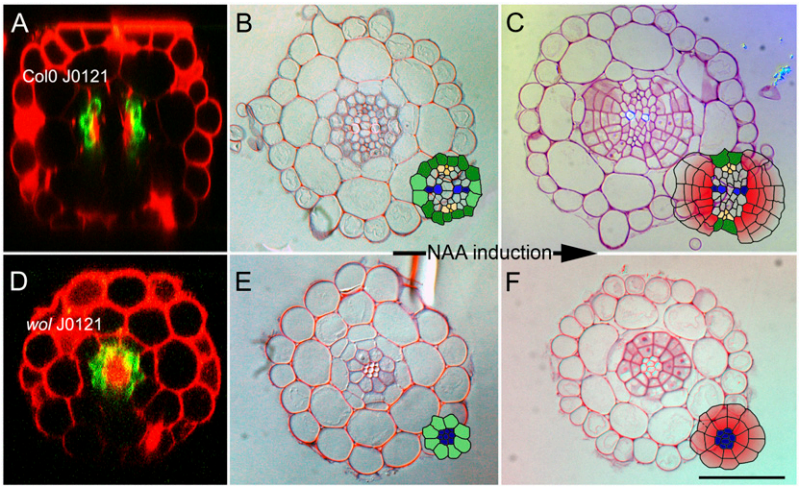

Figure 6. Auxin treatment on *wol* mutant. Col-0 J0121 (A–C) and *wol* J0121 (D–F) have been cultivated (A, B, D, and E) 3 DAG on nonsupplemented medium and then transferred (C and F) 48 h on supplemented medium with 10^{-5} M NAA. Bar = 50 μm.

D), suggesting that all pericycle cells differentiate in only one type of tissue in the mutant background. Furthermore, *wol* can be described as a nonrooting mutant because it makes almost no lateral roots. The ability of *wol* to produce lateral roots under NAA treatment was tested (Fig. 6); no organized primordia were observed above the root tip after 48-h (Supplemental Fig. S5, A–D) or after 96-h (data not shown) treatments as compared with the wild type. Microscope observation of root sections revealed that, in this mutant, all pericycle cells are adjacent to protoxylem elements (Fig. 6E), express GFP (Fig. 6D), are able to divide in a periclinal way upon auxin treatment (Fig. 6F), but do not form primordia.

DISCUSSION

In Arabidopsis, lateral roots originate deep inside the parent root in one layer of cells that surrounds the vascular tissues: the pericycle (Dolan et al., 1993). Only pericycle cells in contact with xylem poles have the competence to initiate lateral root development (De Smet et al., 2006). This process of lateral root initiation occurs above the root tip in the differentiated zone of the root. Competence to form lateral roots is associated with different cell cycle behavior. The pericycle cells adjacent to the xylem poles were shown to continue to divide after leaving the root apical meristem, whereas the other pericycle cells stop dividing (Dubrovsky et al., 2000; Beeckman et al., 2001). Accordingly, xylem pole-associated pericycle cells are shorter than other pericycle cells in the differentiation zone (Beeckman et al., 2001) and differ by their cytological content.

Moreover, the GAL4 enhancer trap line J0121 is specifically expressed in xylem pole-associated pericycle cells, thus suggesting the existence of distinct patterns of gene expression for this subset of cells. However, all these differences between xylem-pole and phloem-pole pericycle cells appear at a distance from the root tip in a mature region of the root where the differentiation of the first vascular elements is fulfilled. This has led to the notion that the lateral root initiation competence of pericycle cells at the xylem poles might rely, to some extent, on correct differentiation of neighboring protoxylem cells. In this view, the lateral root initiation capacity of protoxylem-pole pericycle cells would be a relatively late achieved characteristic. The same train of thought can be found in the earlier reported primed pericycle model (Barlow, 1984; Skene, 2000), wherein all pericycle cells in the root apical meristem are regarded as equivalent and are supposed to differentiate when they leave the meristem in response to a radial factor emitted by differentiated vascular tissues (Fig. 7A). A similar mechanism was demonstrated to control the position of legume nitrogen-fixing nodules in front of xylem poles with ethylene produced in the phloem acting as an inhibitory diffusible factor (Heidstra et al., 1997).

However, in contrast to these hypotheses, our results indicate that the positioning of lateral root primordia is most likely controlled by a different mechanism. We used Rm1007 and J0121 enhancer trap lines and lateral root organogenesis as markers of pericycle cell identity. We show that xylem pole- and phloem pole-associated pericycle cells represent two distinct cell populations with different cellular characteristics. In particular, we observed differential responses of these cells to auxin. Indeed, exogenous treatment with NPA and NAA induces opposite responses between the cells of the pericycle (by blocking division at the xylem poles, whereas the cells in front of phloem poles dedifferentiate and even appear able to divide). This suggests that these two kinds of pericycle cells might have differences in the auxin transport system and/or auxin sensitivity. However, no data have been available to support this hypothesis.

We demonstrate using enhancer trap lines that these two types of pericycle cells might become specified as

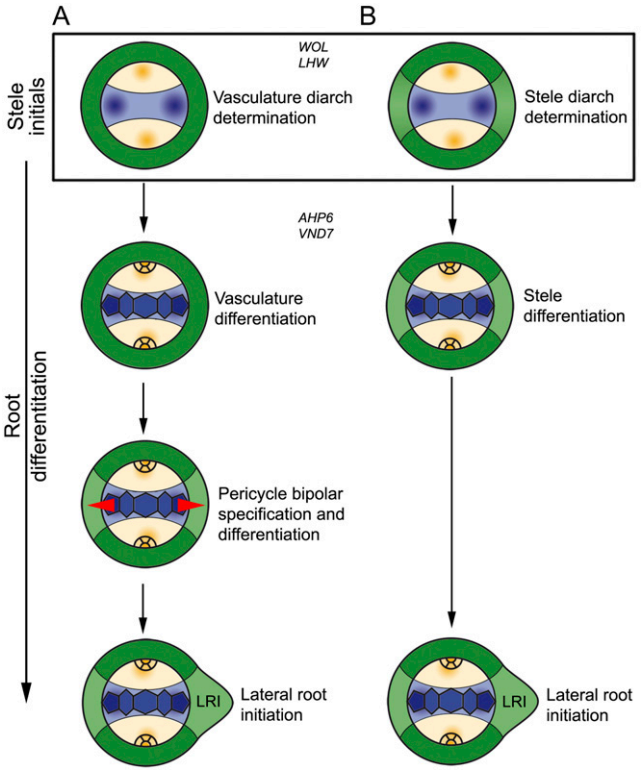

Figure 7. Model for stele determination and differentiation in Arabidopsis. The model (A) proposed previously (Barlow, 1984; Skene, 2000) introduced the diarch organization of the vascular bundle that becomes determined at the level of stele initials. The differentiation of the vascular tissues will later induce the bipolar specification of the pericycle and the differentiation into different cell populations, one of which is associated with the xylem pole and competent for lateral root initiation. Here, we propose an alternative model (B) in which the diarch organization affecting both the vascular bundle and the pericycle is determined from the stele initials onward. The capacity of pericycle cells to give rise to lateral root primordia occurs later and remains associated with vascular tissue differentiation. Blue and orange, respectively, represent xylem and phloem tissues. Green represents the pericycle, with cells associated with the xylem (light green) or phloem (darker green) tissues.

early as, or coinciding with, the formation of the pericycle initials. Moreover, our genetic analysis indicates that pericycle and vasculature determination in the root meristem are controlled by common mechanisms. This is notably illustrated by a concomitant reduction of the cell number of the vasculature and the pericycle in *lhw* and *wol* mutants, whereas the external layers present the same number as the wild type (Supplemental Fig. S3; Dolan et al., 1993). The idea that xylem-pole and phloem-pole pericycle cells are associated with their respective neighboring vascular tissue type is supported by molecular and cellular markers shared between vascular tissues and their associated pericycle cells. For instance, AHP6 (Mahonen et al., 2006) is expressed in protoxylem cells and the adjacent pericycle cells from the initials on. Similarly, at the cellular level, AGP distribution is mainly detected along the xylem axis (Majewska-Sawka and Nothnagel, 2000) and symplastic plasmodesmata connections occur mainly between the phloem cells, adjacent sieve elements, and associated pericycle cells (Wright and Oparka, 1997).

Taken together, our data suggest a new model of pericycle organization (Fig. 7B) where the bilateral organization of the stele, including the pericycle, is set up in the initials and maintained throughout the root, as illustrated by the continuous cell files expressing first Rm1007 and later J0121 markers. Stele determination is notably dependent on the activity of the *WOL* and *LHW* genes. Both *wol* and *lhw* mutations induce a concomitant loss of one vascular pole and the associated pericycle. These observations further suggest that the vascular tissue and its associated pericycle would belong to the same morphogenetic field. Later on, the vascular tissues and the pericycle differentiate as illustrated by vessel formation and lateral root initiation competence, respectively. The lateral root initiation defect in *wol* mutant plants can be either a direct consequence of defects in cytokinin signaling or a result from the loss of the heterogeneity of the pericycle. Quiescent phloem-pole pericycle cells might be needed to border the area of divisions that is required to get proper organogenesis. We therefore argue for the existence of at least two different pericycle cell identities that are closely associated with the adjacent vascular elements. These tissues might therefore be regarded as a full member of the stele, rather than being considered as one other concentric layer of the root.

MATERIALS AND METHODS

Materials Used

Arabidopsis (*Arabidopsis thaliana* L. Heynh.) ecotype Col-0 and C24 seeds were obtained from the Nottingham Arabidopsis Stock Center. We analyzed the mutants *wol* (Mahonen et al., 2000), *ahp6* (Mahonen et al., 2006), the dominant repression line Pro_{35S}-*VND7*:*SDRX* (Kubo et al., 2005; Col-0 background), and the marker line J0121 (Laplaze et al., 2005; C24 background). We used promoter fusion $P_{CYCB1;1:GUS}$ (Colon-Carmona et al., 1999). Rm1007 was identified in a new screen for GAL4-GFP enhancer trap lines in Col-0 background; 2,000 lines were screened; 380 expressed GFP in the root, 57 at least in the pericycle, and 27 specifically in this tissue layer. Of these 27 lines, two labeled a longitudinal subpopulation of cells in this layer.

Growth Conditions and Treatments

Seeds were surface sterilized and sown on one-half-strength selective Murashige and Skoog medium supplemented with 1% Suc and 0.8% agar (Sigma) on vertically oriented square plates (Greiner Labortechnik). For treatments with NPA (Duchefa) or NAA (Sigma-Aldrich), 10 μM was added to the Murashige and Skoog medium (Murashige and Skoog, 1962). For treatments with cytokinin (6-benzylaminopurine; Sigma-Aldrich), 0.01 μM, 0.1 μM, 0.5 μM, and 1 μM were added to the Murashige and Skoog medium. For treatments with variable concentrations of nutrients, we used medium containing 0.001 mM and 2.5 mM phosphate according to Misson et al. (2004), and 0.01 mM and 1 mM nitrate according to Linkohr et al. (2002). For treatments with Suc, 0, 0.02, and 0.15 M doses were added to the Murashige and Skoog medium. Germination was obtained by incubating agar plates, after sowing, for 2 d at 4°C in the dark and then by transferring them to continuous light (110 μmol m^{-2} s^{-1} cool-white fluorescence light) at 20°C with 70% humidity. Heat shock and drought stress have been carried out, respectively, by exposing plants at 40°C for 2 h or by dehydrating them on Whatman 3MM for 2 h at 22°C and then transferring back onto medium. After transfer, observations were done according to the following time course: 0, 6, 12, and 24 h.

Mutagenesis

J0121 seeds homozygous for the enhancer trap insertion (M0) were chemically mutagenized with 0.25% ethyl methanesulfonate) for 12 h and then washed for 5 min with 0.5 M NaOH. Each of the M1 plantlets was grown independently on soil. The mutant selection was carried out on M2 plantlets grown in vitro on one-half-strength selective Murashige and Skoog medium and screened for GFP patterning with a fluorescence stereomicroscope MZFLIII (Leica). Allelism of the mutants was tested by crossing them together and by phenotyping the progeny.

Root Length Measurements

Root length was measured from digital images of the plates using National Institutes of Health ImageJ 1.34S software (http://rsb.info.nih.gov/ij). Emerged lateral roots were counted using a Leica MZ16 binocular microscope. Experiments were repeated at least two times independently.

Histochemical, Histological, and Microscopic Analysis

For whole-mount microscopic analysis, samples were cleared by mounting in a 90% solution of lactic acid (Acros Organics). All samples were analyzed by DIC microscopy (DMLB; Leica Microsystems). For anatomical analysis using light microscopy, transverse sections of roots were performed as described by De Smet et al. (2004). For TEM analysis, samples were treated according to Himanen et al. (2002). For fluorescence microscopy, whole seedlings were stained with 10 μg/mL propidium iodide (Sigma-Aldrich) and mounted in water under glass coverslips for GFP and signal analyzed with a 100 M confocal microscope equipped with software package LSM 510 Version 3.2 (Zeiss). Images were collected with a 488-nm emission filter. For stereomicroscopy, whole seedlings were stained with 10 μg/mL propidium iodide (Sigma-Aldrich) for 3 min and observed with a stereo fluorescence microscope (MZFLIII; Leica).

Supplemental Data

The following materials are available in the online version of this article.

Supplemental Figure S1. Cytokinin treatments on J0121 and NPA/NAA treatments on Rm1007.

Supplemental Figure S2. Mutagenesis mutant root measurements.

Supplemental Figure S3. Cell numbers in the wild type compared with *lhw* and *wol* mutants.

Supplemental Figure S4. Confocal characterization of GFP expression in *lhw* mutants.

Supplemental Figure S5. *wol* pericycle divisions upon NAA treatment.

ACKNOWLEDGMENTS

We thank Dr. M. Kubo for providing *Pro*$_{35S}$*-VND7*:*SDRX*, and Dr. S. Svistoonoff (Equipe Rhizogenèse, IRD Montpellier), L. Jansen (Root Development Group, VIB Ghent), and A.P. Mähönen (Utrecht University) for critical reading of the manuscript.

Received August 23, 2007; accepted November 1, 2007; published November 9, 2007.

LITERATURE CITED

Barlow P (1984) Positional controls in root development. *In* PW Barlow, DJ Carr, eds, Positional Controls in Plant Development. Cambridge University Press, Cambridge, UK, pp 281–318

Beeckman T, Burssens S, Inzé D (2001) The peri-cell-cycle in Arabidopsis. J Exp Bot **52:** 403–411

Casero P, Casimiro I, Knox J (1998) Occurrence of cell surface arabinogalactan-protein and extensin epitopes in relation to pericycle and vascular tissue development in the root apex of four species. Planta **204:** 252–259

Casero PJ, García-Sánchez C, Lloret PG, Navascués J (1989) Changes in cell length and mitotic index in vascular pattern-related pericycle cell types along the apical meristem and elongation zone of the onion root. Protoplasma **153:** 85–90

Casimiro I, Beeckman T, Graham N, Bhalerao R, Zhang H, Casero P, Sandberg G, Bennett MJ (2003) Dissecting Arabidopsis lateral root development. Trends Plant Sci **8:** 165–171

Celenza JL Jr, Grisafi PL, Fink GR (1995) A pathway for lateral root formation in Arabidopsis thaliana. Genes Dev **9:** 2131–2142

Colon-Carmona A, You R, Haimovitch-Gal T, Doerner P (1999) Technical advance: spatio-temporal analysis of mitotic activity with a labile cyclin-GUS fusion protein. Plant J **20:** 503–508

Complainville A, Brocard L, Roberts I, Dax E, Sever N, Sauer N, Kondorosi A, Wolf S, Oparka K, Crespi M (2003) Nodule initiation involves the creation of a new symplasmic field in specific root cells of Medicago species. Plant Cell **15:** 2778–2791

De Smet I, Chaerle P, Vanneste S, De Rycke R, Inzé D, Beeckman T (2004) An easy and versatile embedding method for transverse sections. J Microsc **213:** 76–80

De Smet I, Tetsumura T, De Rybel B, Frey NF, Laplaze L, Casimiro I, Swarup R, Naudts M, Vanneste S, Audenaert D, et al (2007) Auxin-dependent regulation of lateral root positioning in the basal meristem of Arabidopsis. Development **134:** 681–690

De Smet I, Vanneste S, Inzé D, Beeckman T (2006) Lateral root initiation or the birth of a new meristem. Plant Mol Biol **60:** 871–887

Dolan L, Janmaat K, Willemsen V, Linstead P, Poethig S, Roberts K, Scheres B (1993) Cellular organisation of the Arabidopsis thaliana root. Development **119:** 71–84

Dolan L, Roberts K (1995) Secondary thickening in roots of Arabidopsis thaliana: anatomy and cell surface changes. New Phytol **131:** 121–128

Dubrovsky JG, Doerner PW, Colon-Carmona A, Rost TL (2000) Pericycle cell proliferation and lateral root initiation in Arabidopsis. Plant Physiol **124:** 1648–1657

Hardham AR, Gunning BE (1979) Interpolation of microtubules into cortical arrays during cell elongation and differentiation in roots of Azolla pinnata. J Cell Sci **37:** 411–442

Heidstra R, Yang WC, Yalcin Y, Peck S, Emons AM, van Kammen A, Bisseling T (1997) Ethylene provides positional information on cortical cell division but is not involved in Nod factor-induced root hair tip growth in Rhizobium-legume interaction. Development **124:** 1781–1787

Himanen K, Boucheron E, Vanneste S, de Almeida Engler J, Inzé D, Beeckman T (2002) Auxin-mediated cell cycle activation during early lateral root initiation. Plant Cell **14:** 2339–2351

Kubo M, Udagawa M, Nishikubo N, Horiguchi G, Yamaguchi M, Ito J, Mimura T, Fukuda H, Demura T (2005) Transcription switches for protoxylem and metaxylem vessel formation. Genes Dev **19:** 1855–1860

Kurup S, Runions J, Kohler U, Laplaze L, Hodge S, Haseloff J (2005) Marking cell lineages in living tissues. Plant J **42:** 444–453

Laplaze L, Parizot B, Baker A, Ricaud L, Martiniere A, Auguy F, Franche C, Nussaume L, Bogusz D, Haseloff J (2005) GAL4-GFP enhancer trap lines for genetic manipulation of lateral root development in Arabidopsis thaliana. J Exp Bot **56:** 2433–2442

Linkohr BI, Williamson LC, Fitter AH, Leyser HM (2002) Nitrate and phosphate availability and distribution have different effects on root system architecture of Arabidopsis. Plant J **29:** 751–760

Lohar DP, Schaff JE, Laskey JG, Kieber JJ, Bilyeu KD, Bird DM (2004) Cytokinins play opposite roles in lateral root formation, and nematode and rhizobial symbioses. Plant J **38:** 203–214

Mahonen AP, Bishopp A, Higuchi M, Nieminen KM, Kinoshita K, Tormakangas K, Ikeda Y, Oka A, Kakimoto T, Helariutta Y (2006) Cytokinin signaling and its inhibitor AHP6 regulate cell fate during vascular development. Science **311:** 94–98

Mahonen AP, Bonke M, Kauppinen L, Riikonen M, Benfey PN, Helariutta Y (2000) A novel two-component hybrid molecule regulates vascular morphogenesis of the Arabidopsis root. Genes Dev **14:** 2938–2943

Majewska-Sawka A, Nothnagel EA (2000) The multiple roles of arabinogalactan proteins in plant development. Plant Physiol **122:** 3–10

Malamy JE (2005) Intrinsic and environmental response pathways that regulate root system architecture. Plant Cell Environ **28:** 67–77

Misson J, Thibaud MC, Bechtold N, Raghothama K, Nussaume L (2004) Transcriptional regulation and functional properties of Arabidopsis Pht1;4, a high affinity transporter contributing greatly to phosphate uptake in phosphate deprived plants. Plant Mol Biol **55:** 727–741

Murashige T, Skoog F (1962) A revised medium for rapid growth and bioassays with tobacco tissue cultures. Plant Physiol **15:** 473–497

Ohashi-Ito K, Bergmann DC (2007) Regulation of the Arabidopsis root vascular initial population by LONESOME HIGHWAY. Development **134:** 2959–2968

Reed RC, Brady SR, Muday GK (1998) Inhibition of auxin movement from the shoot into the root inhibits lateral root development in Arabidopsis. Plant Physiol **118:** 1369–1378

Scheres B, Di Laurenzio L, Willemsen V, Hauser MT, Janmaat K, Weisbeek P, Benfey PN (1995) Mutations affecting the radial organisation of the Arabidopsis root display specific defects throughout the embryonic axis. Development **121:** 53–62

Scheres B, Wolkenfelt H, Willemsen V, Terlouw M, Lawson E, Dean C, Weisbeek P (1994) Embryonic origin of the Arabidopsis primary root and root meristem initials. Development **120:** 2475–2487

Skene KR (2000) Pattern formation in cluster roots: some developmental and evolutionary considerations. Ann Bot (Lond) **85:** 901–908

Toriyama H (2005) On the remarkable phenomena in the root tip of leguminous plants. Root Research **14:** 35–40

Torrey JG (1950) The induction of lateral roots by indole acetic acid and root decapitation. Am J Bot **37:** 257–264

Vanneste S, De Rybel B, Beemster GT, Ljung K, De Smet I, Van Isterdael G, Naudts M, Iida R, Gruissem W, Tasaka M, et al (2005) Cell cycle progression in the pericycle is not sufficient for SOLITARY ROOT/IAA14-mediated lateral root initiation in *Arabidopsis thaliana*. Plant Cell **17:** 3035–3050

Wright KM, Oparka KJ (1997) Metabolic inhibitors induce symplastic movement of solutes from the transport phloem of Arabidopsis roots. J Exp Bot **48:** 1807–1814